DOI: https://doi.org/10.4038/engineer.v58i2.7698
ENGINEER - Vol. LVIII, No. 02, pp. [113-118], 2025
© The Institution of Engineers, Sri Lanka

Effect of a Notch on the Fatigue Strength of a Gear Shaft

H. M. Asanjitha Jayasekara and S. D. Rasika Perera

Abstract: A failure of a gear shaft in an industrial application led to this investigation. The fractographic analysis revealed that the shaft was subjected to a high stress gradient at the failed location. Finite Element Analysis revealed that the nominal stress was way below the endurance limit of the material, however, due to the design of the shaft, a stress relief groove was used at a point where the shaft diameter had an abrupt change. The relief groove was necessary to properly fit the bearing on the shaft. The stress relief groove acted as a stress riser at the location. This was further verified by an experimental investigation of the stress gradient when in operation, optical imaging of the failed section and further a numerical analysis. A fracture mechanics analysis was used to assess the fatigue life of the notched component.

Keywords: Fatigue, Crack initiation, Fracture mechanics, Fractography

1. Introduction

Shafts are considered as one of the key machine components that are subjected to torsional, axial and bending loads. However, power transmitting shafts are predominantly subjected to torsional loads [1]. Depending on the application, most of these loads are cyclic in nature. Repeated action of cyclic stresses over a period above the endurance limit leading to a final failure is called fatigue failure. Reasons for the application of cyclic stresses above the endurance limit can be poor design, overloading of machines and misalignment of machine components. Even though, the design and manufacture of mechanical components have improved over the period, machine component failures can still be seen in the industry environment. Analysis of the cause and effect of such components is important to identify the reasons and to improve and prevent similar failures in the future. This may further lead to a reduction of downtime and also to prevent damage to factory installations.

The current investigation involves the failure analysis of a gear shaft connected to a rubber sheet processing machine. The objective of the research is to prevent such failures in the future in the industry environment

2. Initial Observations

The shaft was from a hard rubber processing plant where the machine was used to chop the rubber into small pieces. The chopper was driven by an electric motor connected through a gear drive. The output gear shaft was connected to the chopper via a chain drive as shown in Figure 1.

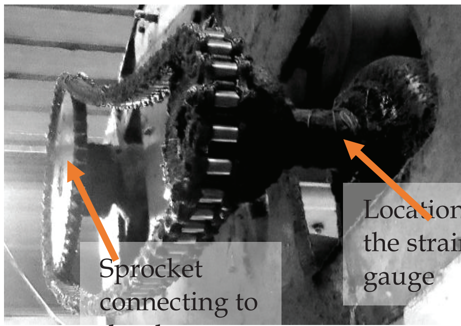

Figure 1 – Connection of the output shaft to the chopper

A pictorial view of the failed gear shaft is shown in Figure 2 and the design of the shaft with dimensions is shown in Figure 3. The initial investigation revealed that the shaft had broken from the location where a relief groove had been provided for stress relief near the bearing seating. Further, it is noted that there is an abrupt change in the diameter from 52 mm to 40 mm in this location.

Eng. H.M. Asanjitha Jayasekara, AMIE(SL), A.Eng.(ECSL), B.Sc. Eng. (Hons) (OUSL), Mechanical Design Engineer, Dragon Arrow (Pvt)Ltd,
Email:masanjitha3@gmail.com
ORCID ID: https://orcid.org/0009-0001-5774-4540
***Dr. S.D. Rasika Perera**, PhD, MPhil, MSc,*
Senior Lecturer in Mechanical Engineering, The Open University of Sri Lanka,
Email:sdper@ou.ac.lk
ORCID ID: https://orcid.org/0000-0001-8516-5768

The stress concentration near the relief groove would also be more due to the abrupt change in diameter from 52 mm to 40 mm [2] at the vicinity of the notch.

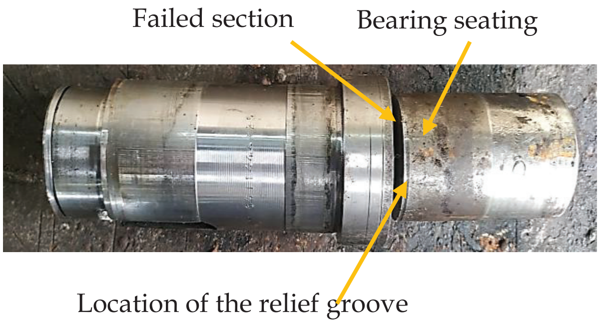

Figure 2 – The failed section and the location of bearing seating on the failed shaft

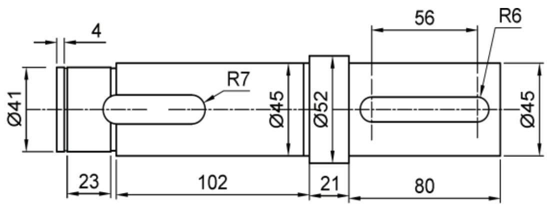

Figure 3 – The dimensions of the failed gear shaft in mm

The location of the failed shaft within the gear box is shown in Figure 4.

The fracture surface is shown in Figure 5. A fatigue fracture surface consists of three zones: the crack initiation zone, the fatigue zone, and the final failure zone due to overload [3].

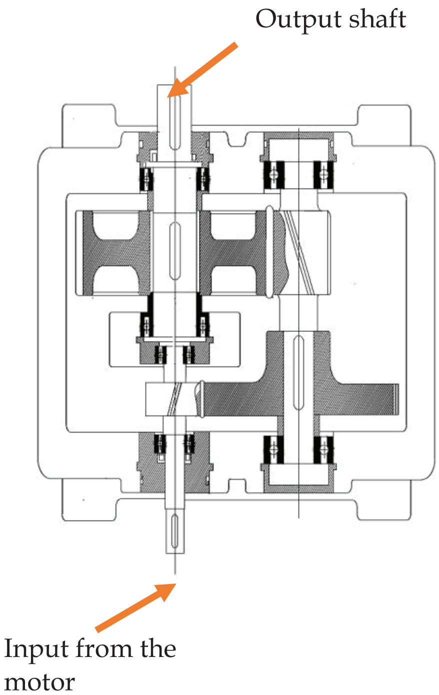

Figure 4 – Schematic diagram of the gear box

A closer examination of the fracture surface reveals ratchet marks in the periphery of the shaft. It is evident from these ratchet marks that the shaft was heavily loaded, and the failure is due to crack initiation in the circumference of the shaft and subsequent failure due to fatigue [4].

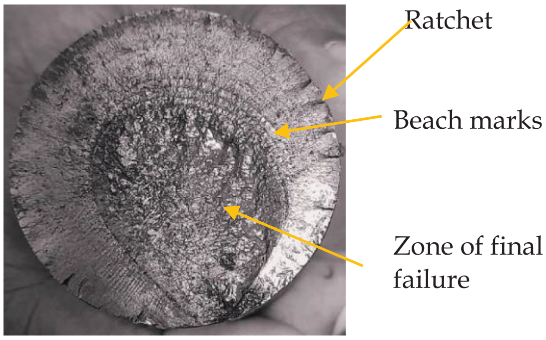

Figure 5 – The failure section of the shaft

3. Methodology

After the failure, the shaft was replaced by an identical shaft. An experimental investigation was carried out on the repaired machine, to assess the stress state the shaft was subjected to during operation. A rosette type strain gauge was used to measure the equivalent stress. The details of instrumentation used to measure the stress is shown in Figure 6.

As it was necessary to measure the actual load applying to the shaft during operation, the reading of the strain gauge was transmitted remotely via Wi-Fi to a computer via a battery powered data acquisition system. The instrumentation connected to the shaft was powered by means of a battery cell, allowing the shaft to rotate freely. The configuration of the data acquisition system is shown in Figure 6.

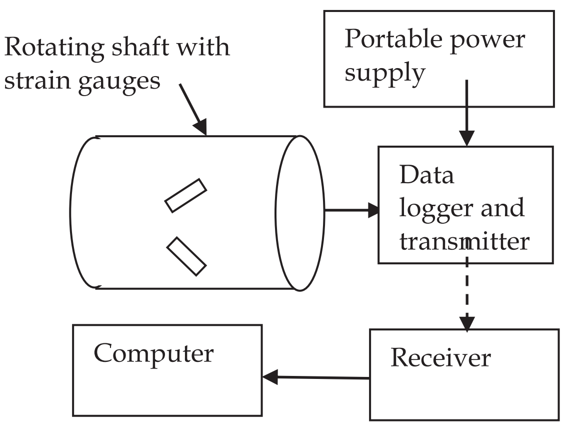

Figure 6 – Configuration of the data acquisition system

The strain bridge was calibrated prior to the experiment. The data was logged to a computer remotely while the machine was in operation. The data was further refined by obtaining the average for further analysis.

4. Results

The torque vs time graph plotted from the acquired data is shown in Figure 7. The speed of rotation of the shaft was 13 rev/min.

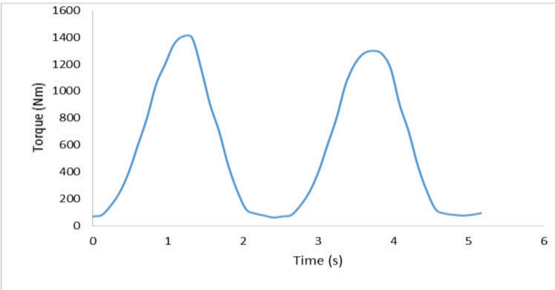

Figure 7 – Torque vs time graph for the shaft

The torsional moment depicted in Figure 7 reveals that the shaft is subjected to a cyclic torsional moment. The fact that the shaft was operating at a high torsional moment was evident from the ratchet marks visible closer to the surface of the shaft. The peak moment recorded was 1408 Nm.

.

The material properties of the shaft were estimated by carrying out a tensile test. The result of the tensile test is shown in Figure 8.

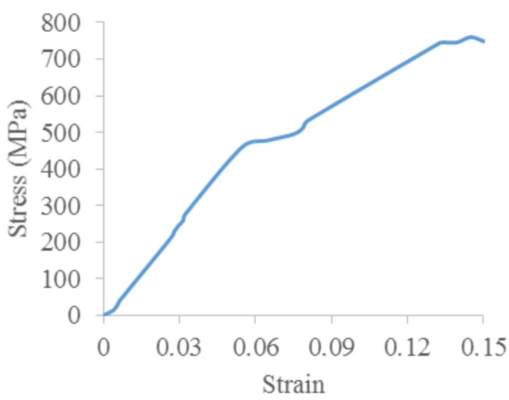

Figure 8 – Tensile test of the material

The material was of yield strength 460MPa and ultimate tensile strength 748MPa. The hardness profile across a section at the vicinity of the failed section is shown in Figure 9. The variation of the harness profile reveals that the surface of the shaft had not been heat treated.

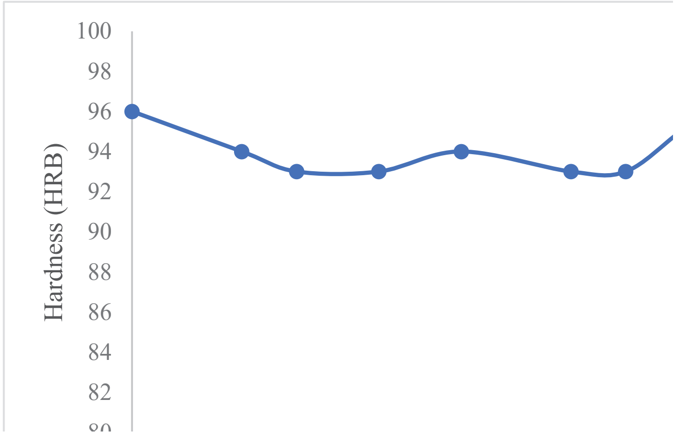

Figure 9 - The hardness profile

The microstructure was analysed using optical microscopy. The typical microstructure shown in Figure 10 depicts that the microstructure consists of ferrite pearlite alloy steel.

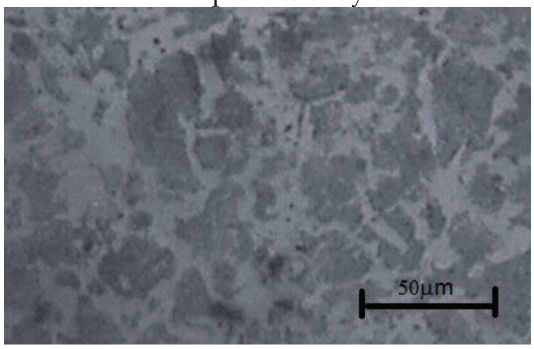

Figure 10 – Microstructure of the shaft

The chemical composition of the material was tested using Arc-Spark Optical Emission Spectroscopy. The composition of the shaft is given in Table 1. It was found that the physical properties, microstructure and the chemical composition coincide with that of SAE1042 material [3].

Table 1 - Chemical composition of the tested material and equivalent standard material

Composition	C	Si	Mn	Cr
Tested material	0.3	0.33	0.59	0.12
SAE 1042	0.35-0.4	0.1 – 0.35	0.5-1.2	

A finite element analysis was carried out using Solidworks software in order to assess the stress distribution throughout the shaft during real life operation.

As it was necessary to interpret the yield strength obtained by the uniaxial stress for complex loading conditions, the Von Mises stress criterion was used for the analysis. The Von Mises stress determines an equivalent stress that is used to determine if a material will begin to yield. According to the Von Mises criteria, a material will not yield if the maximum von Mises stress value does not exceed the yield strength of the material.
The boundary condition applied to the shaft and the location of torque application is shown in Figure 11.

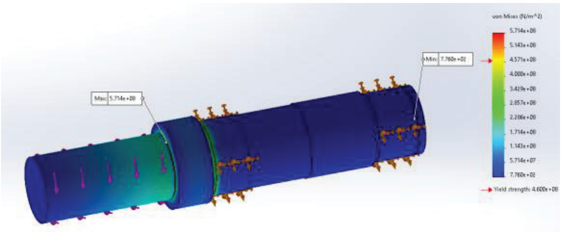

Figure 11 - FEM Analysis results with constraints and application of moment

The simulation of the shaft under an equivalent moment of 1408 Nm was conducted using three different mesh densities, employing the standard triangular mesh type for element size of 12 mm, 8 mm, 6 mm, 5mm, 3.4mm and 3 mm. The mesh sensitivity analysis revealed that the mesh size of 3.4 mm leads to convergence. This refined mesh configuration was implemented to enhance the accuracy of the stress distribution analysis by capturing finer details of the stress variations while ensuring numerical stability.

5. Analysis

The visual inspection revealed that the failure had occurred in the vicinity of the relief groove. The FEM analysis also revealed that the highest local stress gradient is present near the relief groove. The local stress field recorded a maximum of 490 MPa.

A fracture mechanics based analysis was carried out in order to assess the effect of local stress gradient on the fatigue strength of the shaft. It has been noted that the failure has occurred at the stress relief groove at the bearing seat. The variation of the hardness profile confirms that the shaft has not been heat treated. The stress relief groove can be assumed to be a notch in terms of stress gradient along the shaft.

The analysis is based on determining the fatigue strength of the notched component at 1, 1000 and 1000,000 cycles.

The theoretical stress concentration factor k_t at the notch can be written as [5]

$$k_t = \frac{\sigma_{\max}}{s} \quad \ldots(1)$$

where, $\sigma_{\max}$ is the maximum stress at the notch and s is the nominal stress on the shaft at the lowest sectional diameter. The nominal stress was found to be 127 MPa and the maximum stress σ_{max} determined from the FEM analysis was 490 MPa. Then the stress concentration factor, k_t was found to be $k_t = \frac{490}{127} = 3.89$

In the stress life approach, the effect of the notch is accounted for by comparing the plain fatigue strength to that of a notched member at a given life. This ratio is identified as fatigue notch factor as given in equation (2).

$$k_f = \frac{s_e^{unnotched}}{s_e^{notched}} \quad \ldots(2)$$

where $s_e^{unnotched}$ is the endurance limit of the unnotched member and $s_e^{notched}$ is the endurance limit of notched member. Even though the stress concentration factor is governed by the stress gradient and mode of loading, the fatigue notch factor depends on material properties in addition to the stress gradient and mode of loading. An additional parameter, notch sensitivity factor q, has been developed to link the stress concentration factor and stress intensity factor, via equation (3).

$$q = \frac{k_{f-1}}{k_{t-1}} \quad \ldots(3)$$

Further, Peterson [6] proposed an empirical relationship to determine the notch sensitivity factor as:

$$q = \frac{1}{\left(1 + \frac{a}{r}\right)} \quad \ldots(4)$$

where, r is notch root radius and a is a material constant called as Neuber's constant. By combining both equations, it can be shown that

$$k_f = 1 + \frac{k_t - 1}{\left(1 + \frac{a}{r}\right)} \quad \ldots(5)$$

The value a was determined by referring to the relevant table given in [5]. In the table, a corresponding value is given based on the Ultimate Tensile Strength (UTS) of the material. It is advised to keep in mind that these key equations have been developed for empirical units and values obtained in SI units are required to be converted appropriately. The UTS of the material used to fabricate the shaft under investigation was 748 MPa, which is 108.5 ksi. The corresponding value of $\sqrt{a}$ for 108.5 ksi is 0.055 inch. Further, the notch radius measured by means of talysurf was converted to inches. When values have been substituted into equation (5),

$$k_f = 1 + \frac{4.45 - 1}{\left(1 + \frac{(0.55)^2}{0.019}\right)} = 3.49$$

k_f= 3.49 for life estimation purposes, k_f is considered as the fatigue stress intensity factor at 10^6 cycles [5].

Next, the fatigue stress concentration factor at 1000 cycles, k'_f, is determined. The ultimate tensile strength of the material was determined from a tensile test was 748 MPa = 108.5 ksi. The corresponding q value of the graph proposed by Juvinall [7] as given in [5] for 108.5 ksi is 0.22. Then

$$q = \frac{k'_f - 1}{k_f - 1} = 0.22$$

Substituting value of k_f and q, k'_f can be determined as:

$$k'_f = (3.49 - 1)0.22 + 1 = 1.54$$

Next the endurance limit of the material was estimated. The endurance limit of the material can be assumed to be as shown in equation (6) [5].

$$s_e = 0.5Su \qquad \ldots(6)$$

Substituting values,

$$s_e = 0.5(92.8) = 54.2ksi$$

Next, determine the stress level corresponding to 1000 cycles.

The fatigue strength at 1000 cycles can be assessed by equation (7) [5].

$$s_{1000} = 0.9Su \qquad \ldots(7)$$

Substituting values,

$$s_{1000} = 0.9(92.8) = 83.6ksi,$$

Based on the above estimates, now the fatigue strength of the notched component can be determined.

The estimation has been recommended only for comparison purposes and should not be used for design purposes [5].

Previously, k'_f and , k_f, which correspond to the fatigue stress intensity factor at 1000 cuc;es amd 10^6 cycles, respectively, for the notched component were determined.

Now, the fatigue strength for the notched component at 1000 cycles is given by the ratio $\frac{s_{1000}}{k'_f}$ and the fatigue strength at 10^6 cycles is given by $\frac{s_e}{k_f}$.

The estimated fatigue strength at one cycle is the true fracture strength. For steel, this can be approximated as Su+50 ksi [5]. The UTS of the material was 748 MPa. The magnetide in ksi is equivalent to 108.5 ksi.

The calculations are being presented in Table 2.

Table 2 – Parameters for the modified SN curve for notched component

No of cycles	Formula	Value in ksi	Value in MPa
10^6 cycles	$\frac{s_e}{k_f}$	$\frac{54.2}{3.49} = 15.5$	106.8
10^3 cycles	$\frac{s_{1000}}{k'_f}$	$\frac{83.6}{1.54} = 54.2$	373
1 cycle	Su+50	108.5+50=158.5	1092

The modified fatigue curve for the notched component is given in Figure 12.

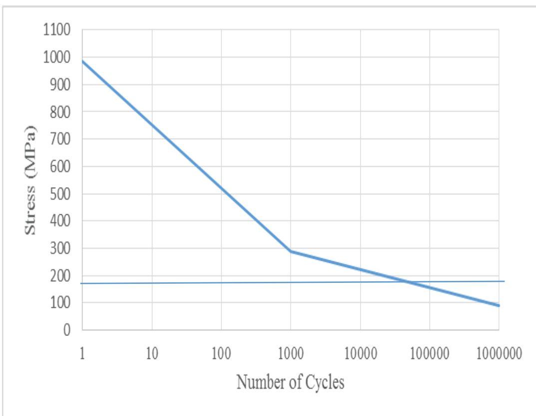

Figure 12 - S N curve for the notched component

6. Discussion and Conclusions

The fractographic image shows that the shaft has been heavily loaded and subjected to high stress concentration.

This was evident from the multiple ratchet marks spread almost all over the periphery at the broken section. Further, the FEM analysis revealed that a severe stress gradient exists at the location of the relief groove provided for the bearing, which is also a stress concentration.

The ratchet marks provide evidence of crack initiation on several locations simultaneously due to stress concentration at the relief groove. Figure 3 depicts clearly that cracks that have been initiated at different locations have propagated inward across the section. The nominal stress at the smallest diameter section was found to be less than the endurance limit of the material. However, the notched endurance limit for the material is 193 MPa, which is lower than the highest recorded stress near the relief groove.

A fracture analysis was carried out for the notched condition at the relief groove. The modified fatigue curve developed to replicate the scenario. The intersecting point of the nominal stress at the lowest diameter section on the modified SN curve shown in Figure 12 reveals that the component fails due to fatigue in less than 1000,000 cycles. Analysis revealed that, if the output shaft was rotating at 13 rpm for 8 hours per day for 250 days per year, the shaft would have failed in less than one year of operation. The shaft has been overloaded in the current application.

Whilst the nominal stress is way below the yield stress, presence of a notch could increase localised stresses which could lead to a failure.

Acknowledgements

Authors wish to acknowledge the contribution of Mr. Sirira Kumara, Mr. K. C. K. Deraniyagala and Mrs. Anusha Waijayanthi for their contribution.

References

1. Chai, H. Y., Lee, S, "Stability of Structures". (2011). *Elsevier eBooks*. Elsevier BV. doi:https://doi.org/10.1016/c2010-0-66075-5.

2. Pilkey, W. D. and Pilkey, D. F. (2008). "*Peterson's Stress Concentration Factors*". Hoboken: John Wiley, Cop.

3. ASM International. (1996). "Failure Analysis and Prevention" Vol. 11. Metals Park (OH): *American Society for Metals*; 1996.

4. Affonso, L.O.A. (2013). "*Machinery Failure Analysis Handbook: Sustain Your Operations and Maximize Uptime*". Burlington: Elsevier Science.

5. Bannantine, J. A., Comer, J. J. and Handrock, J. L. (1990). "*Fundamentals of Metal Fatigue Analysis*". Pearson.

6. Peterson, R. E. (1945) "Relation between life testing and conventional tests of materials" *Bulletin ASTM No 133*, 1945.

7. Juvinall, R. C. (1967), "Engineering Considerations of Stress, Strain and Strength, McGraw Hill, New York, 1967.

.